J|A|C|S
ARTICLES
Published on Web 10/20/2005

A Multi-Mode-Driven Molecular Shuttle: Photochemically and Thermally Reactive Azobenzene Rotaxanes

Hiroto Murakami,[†] Atsushi Kawabuchi,[†] Rika Matsumoto,[†] Takeshi Ido,[†] and Naotoshi Nakashima*[,‡]

Contribution from the Department of Applied Chemistry, Faculty of Engineering, Nagasaki University, Nagasaki 852-8521, Japan, and Department of Chemistry and Biochemistry, Graduate School of Engineering, Kyushu University, Fukuoka 812-8581, Japan

Received June 21, 2005; E-mail: nakashima-tcm@mbox.nc.kyushu-u.ac.jp

Abstract: The shuttling process of α-CyD in three rotaxanes (**1**−**3**) containing α-cyclodextrin (α-CyD) as a ring, azobenzene as a photoactive group, viologen as an energy barrier for slipping of the ring, and 2,4-dinitrobenzene as a stopper was investigated. The *trans*−*cis* photoisomerization of **1** by UV light irradiation occurred in both DMSO and water due to the movement of α-CyD toward the ethylene group, while the photoisomerization of **2** occurred in DMSO, but not in water. No photoisomerization was observed for **3** in both water and DMSO. The activation parameters of **1** and **1-ref** in DMSO are subject to a compensation relation between $\Delta S^{\ddagger}$ and $\Delta H^{\ddagger}$; however, in water, the $\Delta S^{\ddagger}$ terms are not compensated by the $\Delta H^{\ddagger}$ terms. Alternating irradiation of the UV and visible lights resulted in a reversible change in the induced circular dichroism (ICD) bands of *trans*-**1** and *cis*-**1**. In contrast, after the UV light irradiation, the ICD band of *trans*-**2** decreased without the appearance of any bands of *cis*-**2**. The NMR spectra of **2** in DMSO showed coalescence of the split signals for the methylene and for the viologen protons due to the shuttling of α-CyD. Both the NOE differential spectra for *cis*-**1** in water after UV light irradiation and **2** in DMSO after heating to 120 °C showed the negative NOE peaks assigned to interior protons of α-CyD, suggesting that α-CyD in *cis*-**1** exists at the one ethylene moiety, and α-CyDs in *cis*-**2** and **2** heated in DMSO exist at the propylene moieties.

Introduction

The construction of artificial devices and machines, both of which function with external stimuli at the molecular level, has attracted much attention in the nanoscience and nanotechnology areas.[1−5] Rotaxanes and catenanes, in which two or more molecular components are mechanically interlocked, are suitable candidates for the construction of molecular devices and machines.[6] Particularly, since the first proposal by Stoddart and co-workers in 1991,[7] molecular shuttles based on the rotaxane structure, in which the shuttling process of a ring is controlled by external stimuli, have been widely studied as one type of molecular machines. Since the first molecular shuttle,[7] many different types of rotaxanes have been synthesized, and heat,[7−18] pH,[11,19−22] redox,[11,22−26] ion addition,[17,27] solvent polarity,[12,14,16,28,29] and light[13,14,21,23,28,30−38] have been used as external stimuli, of which heat and light are the most convenient way to

[†] Nagasaki University.
[‡] Kyushu University.

(1) Balzani, V.; Credi, A.; Raymo, F. M.; Stoddart, J. F. *Angew. Chem., Int. Ed.* **2000**, *39*, 3248−3391.
(2) Ballardini, R.; Balzani, V.; Credi, A.; Gandolfi, M. T.; Venturi, M. *Acc. Chem. Res.* **2001**, *34*, 445−455.
(3) Harada, A. *Acc. Chem. Res.* **2001**, *34*, 456−464.
(4) Schalley, C. A.; Beizai, K.; Vögtle, F. *Acc. Chem. Res.* **2001**, *34*, 465−476.
(5) Collin, J.-P.; Dietrich-Buchecker, C.; Gaviña, P.; Jimenez-Molero, M. C.; Sauvage, J.-P. *Acc. Chem. Res.* **2001**, *34*, 477−487.
(6) Sauvage, J.-P.; Dietrich-Buchecker, C. *Molecular Catenanes, Rotaxanes and Knots*; Wiley-VCH: Weinheim, Germany, 1999.
(7) Anelli, P. L.; Spencer, N.; Stoddart, J. F. *J. Am. Chem. Soc.* **1991**, *113*, 5131−5133.
(8) Lee, J. W.; Kim, K.; Kim, K. *Chem. Commun.* **2001**, 1042−1043.
(9) Chiu, S.-H.; Elizarov, A. M.; Glink, P. T.; Stoddart, J. F. *Org. Lett.* **2002**, *4*, 3561−3564.
(10) Loeb, S. J.; Wisner, J. A. *Chem. Commun.* **2000**, 1939−1940.
(11) Bissell, R. A.; Córdova, E.; Kaifer, A. E.; Stoddart, J. F. *Nature* **1994**, *369*, 133−137.
(12) Anelli, P.-L. et al. *Chem.—Eur. J.* **1997**, *3*, 1113−1135.
(13) Altieri, A.; Bottari, G.; Dehez, F.; Leigh, D. A.; Wong, J. K. Y.; Zerbetto, F. *Angew. Chem., Int. Ed.* **2003**, *42*, 2296−2300.
(14) Bottari, G.; Dehez, F.; Leigh, D. A.; Nash, P. J.; Pérez, E. M.; Wong, J. K. Y.; Zerbetto, F. *Angew. Chem., Int. Ed.* **2003**, *42*, 5886−5889.
(15) Ashton, P. R.; Philip, D.; Spencer, N.; Stoddart, J. F. *J. Chem. Soc., Chem. Commun.* **1992**, 1124−1128.
(16) Asakawa, M.; Brancato, G.; Fanti, M.; Leigh, D. A.; Shimizu, T.; Slawin, A. M. Z.; Wong, J. K. Y.; Zerbetto, F.; Zhang, S. *J. Am. Chem. Soc.* **2002**, *124*, 2939−2950.
(17) Jiang, L.; Okuno, J.; Orita, A.; Otera, J. *Angew. Chem., Int. Ed.* **2004**, *43*, 2121−2124.
(18) Kawaguchi, Y.; Harada, A. *Org. Lett.* **2000**, *2*, 1353−1356.
(19) Cao, J.; Fyfe, M. C. T.; Stoddart, J. F. *J. Org. Chem.* **2000**, *65*, 1937−1946.
(20) Badjić, J. D.; Balzani, V.; Credi, A.; Silvi, S.; Stoddart, J. F. *Science* **2004**, *303*, 1845−1849.
(21) Wang, Q.-C.; Qu, D. H.; Ren, J.; Chen, K.; Tian, H. *Angew. Chem., Int. Ed.* **2004**, *43*, 1661−1665.
(22) Ashton, P. R.; Ballardini, R.; Balzani, V.; Baxter, I.; Credi, A.; Fyfe, M. C. T.; Gandolfi, M. T.; Gómez-López, M.; Martínez-Díaz, M.-V.; Piersanti, A.; Spencer, N.; Stoddart, J. F.; Venturi, M.; White, A. J. P.; Williams, D. J. *J. Am. Chem. Soc.* **1998**, *120*, 11932−11942.
(23) Armaroli, N.; Balzani, V.; Collin, J.-P.; Gaviña, P.; Sauvage, J.-P.; Ventura, B. *J. Am. Chem. Soc.* **1999**, *121*, 4397−4480.
(24) Kihara, N.; Hashimoto, M.; Takata, T. *Org. Lett.* **2004**, *6*, 1693−1696.
(25) Altieri, A.; Gatti, F. G.; Kay, E. R.; Leigh, D. A.; Martel, D.; Paolucci, F.; Slawin, A. M. Z.; Wong, J. K. Y. *J. Am. Chem. Soc.* **2003**, *125*, 8644−8654.
(26) Tseng, H.-R.; Vignon, S. A.; Stoddart, J. F. *Angew. Chem., Int. Ed.* **2003**, *42*, 1491−1495.

10.1021/ja053690l CCC: $30.25

Chart 1

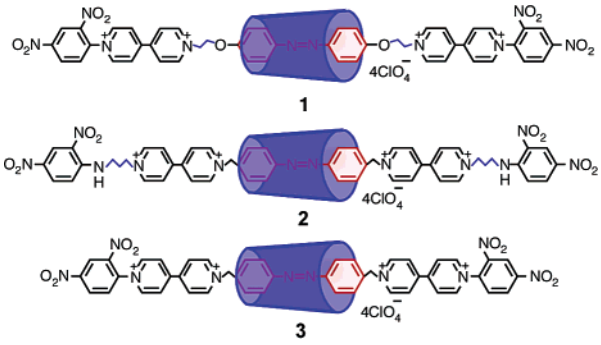

supply energy to the molecular shuttles. Light as the stimulus includes three types of photochemical reactions to drive molecular shuttles, namely, (i) photoinduced electron-transfer, (ii) photoinduced chemical reaction, and (iii) photoisomerization processes. Elegant examples of molecular shuttles driven by photoinduced electron-transfer processes have been reported by several groups.[23,28,30−32,34] Abraham and co-workers described a molecular shuttle driven by a photochemical reaction, in which photoheterolysis was used to switch the position of a tetracationic macrocycle.[35] Azobenzene is a suitable component to construct a molecular shuttle driven by photoisomerization because the *trans*−*cis* photoisomerization of azobenzene induces a drastic change in its molecular occupied volume. We have described the first photodriven molecular shuttling behavior using **1**, which possesses α-CyD as a ring molecule and an azobenzene derivative as a threading molecule, in which α-CyD moves back and forth from/to the azobenzene moiety to/from the ethylene spacer by alternating UV and visible light irradiation.[36] Sohlberg and co-workers carried out AM1 semiempirical electronic structure calculations for the light-driven molecular shuttling behavior of **1**.[39] After our report, the photoisomerization behaviors of an azobenzene,[33,38] a stilbene,[21,37] and a maleamide[14,28,31,32] have been used as the photoisomerization groups.

In the present study, we describe (i) the design and synthesis of two rotaxanes (**2** and **3**) in addition to the previously reported compound **1** (Chart 1), (ii) the isomerization behavior of the azobenzene moieties in these rotaxanes, and then (iii) the light, heat, and solvent polarity-controlled molecular shuttling behaviors using these compounds. In this paper, we discuss the importance of the rotaxane structures for the design of a multimode molecular shuttle. Several dual-mode-driven molecular shuttles[12,13,16,17,21−23] have already been reported; however, the papers describing the triple-mode-driven molecular shuttles[11,14] are very limited. Stoddart and co-workers reported the shuttling processes of a rotaxane that consists of a tetracationic macrocycle and a thread, which possesses a benzidine and a biphenol units as a station that are controlled by three external stimuli, namely, heat, pH, and the redox reaction.[11] Leigh and co-workers described a heat-, light-, and solvent polarity-driven molecular shuttle, in which the benzylic amid macrocycle shuttles between the fumaramide and the maleamide stations.[14]

Results and Discussion

Design and Synthesis. In this study, we use three rotaxanes (**1**−**3**), containing a ring, a primary station as a photoactive unit, and bulky terminal stoppers of α-CyD, azobenzene, viologen, and 2,4-dinitrobenzene. As we previously described,[36] the rotaxane **1** is a short-distance molecular shuttling compound that possesses ethylene spacers as a secondary station next to the azobenzene unit. The rotaxane **2** is a long-distance molecular shuttling compound that possesses propylene spacers as a secondary station on opposite sides across the viologen units from the azobenzene. In contrast, no secondary station exists in the rotaxane **3**; therefore, it is expected that compound **3** does not work as a molecular shuttle.

The synthesis of **1** and its reference compound, **1-ref**, have already been briefly described elsewhere.[36] We now describe the details. The rotaxanes **1**, and **2** and **3** were prepared according to Schemes 1 and 2, respectively. The reaction of **6** with ca. 5 equiv of 4,4′-bipyridyl produced a "thread" compound **7** in 57% yield. The thread compounds **9** and **10** were also obtained by the reaction of 4,4′-bis(chloromethyl)azobenzene[40] with ca. 5 equiv each of **8** and 4,4′-bipyridyl in 86 and 57% yields, respectively. The reactions of **7**, **9**, and **10** with 10−20 equiv of 2,4-dinitrofluorobenzene in the presence of α-CyD, followed by anion exchange from Br^- to ClO_4^- gave rotaxanes **1**, **2**, and **3** in 30, 68, and 4% yields, respectively. The poor yield of **3** might be due to the weak binding between **10** and α-CyD. Reference compounds **1-ref**, **2-ref**, and **3-ref** were synthesized by procedures similar to those of **1**−**3** in the absence of α-CyD, and their yields were 48, 30, and 71%, respectively.

Formation of Rotaxane Structure. As we described in a previous paper,[36] the existence of the threads in the cavity of α-CyD was confirmed by ^{1}H NMR spectroscopy. That is, the chemically equivalent protons on **1-ref** were located in the same electromagnetic environment, which is in sharp contrast to that of **1**, where the split signals with equal intensity[41] appear. This means that the respective protons on **1-ref** are chemically equivalent for C_2 symmetry axis on the azo group, whereas **1** loses the symmetry due to the presence of α-CyD. This result supports the formation of the rotaxane structure for **1**.[36] Similar ^{1}H NMR spectral behavior was observed for **2** and **2-ref** and for **3** and **3-ref**, indicating that both **2** and **3** also form the rotaxane structure. In the spectra of **1**−**3**, the signal of the azobenzene protons next to the azo group splits 0.67, 0.62, and

(27) Vignon, S. A.; Jarrosson, T.; Iijima, T.; Tseng, H.-R.; Sanders, J. K. M.; Stoddart, J. F. *J. Am. Chem. Soc.* **2004**, *126*, 9884−9885.
(28) Bottari, G.; Leigh, D. A.; Pérez, E. M. *J. Am. Chem. Soc.* **2003**, *125*, 13360−13361.
(29) Lane, A. S.; Leigh, D. A.; Murphy, A. *J. Am. Chem. Soc.* **1997**, *119*, 11092−11093.
(30) Benniston, A. C.; Harriman, A. *Angew. Chem., Int. Ed.* **1993**, *32*, 1459−1461.
(31) Pérez, E. M.; Dryden, D. T. F.; Leigh, D. A.; Teobaldi, G.; Zerbetto, F. *J. Am. Chem. Soc.* **2004**, *126*, 12210−12211.
(32) Brouwer, A. M.; Frochot, C.; Gatti, F. G.; Leigh, D. A.; Mottier, L.; Paolucci, F.; Roffia, S.; Wurpel, G. W. H. *Science* **2001**, *291*, 2124−2128.
(33) Kauffmann, C.; Müller, W. M.; Vögtle, F.; Weinman, S.; Abramson, S.; Fuchs, B. *Synthesis* **1999**, 849−853.
(34) Ashton, P. R.; Ballardini, R.; Balzani, V.; Credi, A.; Dress, K. R.; Ishow, E.; Kleverlaan, C. J.; Kocian, O.; Preece, J. A.; Spencer, N.; Stoddart, J. F.; Venturi, M.; Wenger, S. *Chem.*−*Eur. J.* **2000**, *6*, 3558−3574.
(35) Abraham, W.; Grubert, L.; Grummt, U. W.; Buck, K. *Chem.*−*Eur. J.* **2004**, *10*, 3562−3568.
(36) Murakami, H.; Kawabuchi, A.; Kotoo, K.; Nakashima, N. *J. Am. Chem. Soc.* **1997**, *119*, 7605−7605.
(37) Stanier, C. A.; Alderman, S. J.; Claridge, T. D. W.; Anderson, H. L. *Angew. Chem., Int. Ed.* **2002**, *41*, 1769−1772.
(38) Qu, D. H.; Wang, Q.-C.; Ren, J.; Tian, H. *Org. Lett.* **2004**, *6*, 2085−2088.
(39) Sohlberg, K.; Sumpter, B. G.; Noid, D. W. *J. Mol. Struct.* **1999**, *491*, 281−286.
(40) Shinkai, S.; Shigematsu, K.; Kusano, Y.; Manabe, O. *J. Chem. Soc., Perkin Trans. 1* **1981**, 3279−3283.
(41) Sito, H.; Yonemura, H.; Nakamura, H.; Matsuo, T. *Chem. Lett.* **1990**, 535−538.

Scheme 1. Synthesis of Rotaxane **1**[a]

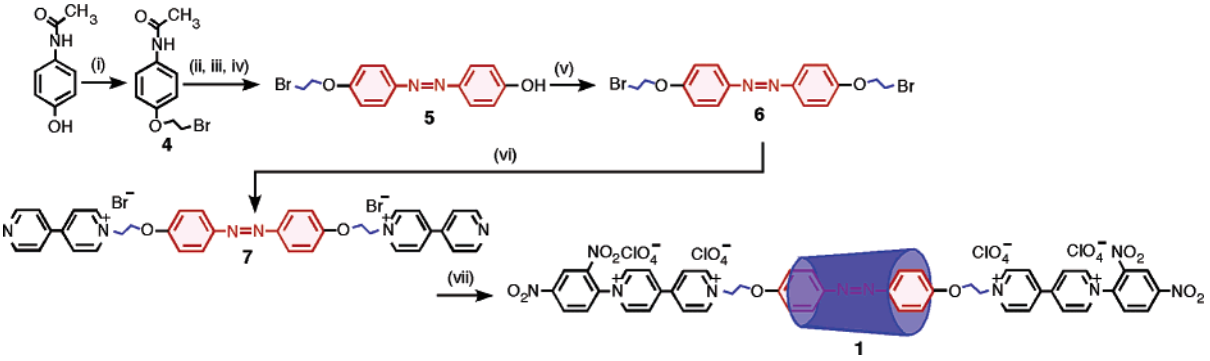

[a] Conditions: (i) 1,2-dibromoethane, Bu_4NClO_4, sat. Na_2CO_3 aq., Δ, 40%; (ii) HBr, EtOH, Δ; (iii) $NaNO_2$, 1 M HCl aq., 0 °C; (iv) phenol, Na_2CO_3, water, 0 °C, 90%; (v) 1,2-dibromoethane, Bu_4NClO_4, sat. Na_2CO_3 aq., Δ, 50%; (vi) 4,4′-bipyridyl, DMF, Δ, 57%; (vii) α-cyclodextrin, 2,4-dinitrofluorobenzene, water, rt, $NaClO_4$ (ion exchange), 30%.

Scheme 2. Synthesis of Rotaxanes **2** and **3**[a]

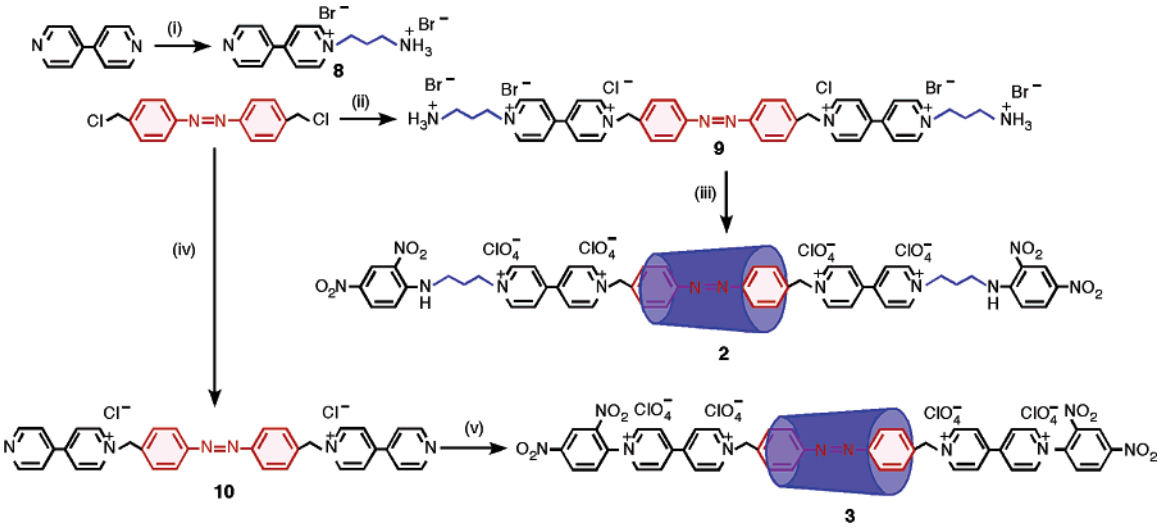

[a] Conditions: (i) 3-bromopropylamine hydrobromide, MeCN, Δ, 58%; (ii) DMSO, Δ, 86%; (iii) α-cyclodextrin, 2,4-dinitrofluorobenzene, water, rt, $NaClO_4$ (ion exchange), 68%; (iv) 4,4′-bipyridyl, DMF, Δ, 57%; (v) α-cyclodextrin, 2,4-dinitrofluorobenzene, water, rt, $NaClO_4$ (ion exchange), 4%.

0.62 ppm for **1**, **2**, and **3** in DMSO, which are larger than those of the other protons. The split values of the signals for the other protons on the rotaxanes gradually decreased with the increase in the distance from the azo group, probably due to the lack of anisotropy produced by α-CyD in **1**. Thus, the obtained NMR results indicate that α-CyD remains at the azobenzene moiety on the rotaxanes. Furthermore, it was found that, in DMSO, the protons of the methylene spacers in **3** produced double-doublet and broad singlet signals, while in D_2O, they gave two sharp singlet signals (see Supporting Information, Figure S1). The ^1H NMR spectrum of **2** in DMSO also showed double-doublet and broad singlet signals for the methylene spacers. The appearance of the double-doublet and broad singlet signals reveals that the geminal protons on one methylene next to the azobenzene in **2** (and **3**) are chemically nonequivalent and those on the other methylene are chemically equivalent. This spectral behavior might be due to the formation of hydrogen bonding[10] between the hydroxy groups on α-CyD and the geminal protons on the one methylene, of which the acidity is enhanced by the electron attractive pyridinium group. The appearance of the induced CD (ICD) for the rotaxanes is also evidence for the formation of the rotaxane structure. More details are described in the section of Molecular Shuttling Driven by Light and Heating.

Photoisomerization and Thermal Isomerization. The *trans*−*cis* photoisomerization followed by *cis*−*trans* thermal isomerization of the azobenzene moiety in the rotaxanes was examined in water and in DMSO. The typical UV−visible spectra of **1** in water and **2** in water and DMSO at the specified temperatures are shown in Figure 2 (A, C, and E, respectively). The *cis*-isomerization ratios are summarized in Table 1. UV light irradiation in aqueous and DMSO solutions of **1** causes the photoisomerization from the *trans*- to *cis*-form of the azobenzene moiety, whereas, as we expected, no photoisomerization of **3** was observed in water and DMSO (see Supporting Information, Figure S2). It is evident that the existence of the ethylene groups in **1** as the secondary station between the azobenzene moiety and the viologen moiety is important for the photoisomerization. That is, α-CyD in **1** is readily movable to the ethylene group. On the other hand, the rotaxane **2** shows the photoisomerization behavior in DMSO; however, in water, the photoisomerization of **2** was almost negligible. It is known that, in water, cationic viologens act as an energy barrier for the slipping of α-CyD due to the energetically unfavorable interaction between α-CyD and the viologen moieties.[41,42] For this reason, α-CyD is expected to locate at the azobenzene moiety in **2** (and **3**). When

(42) Kawaguchi, Y.; Harada, A. *J. Am. Chem. Soc.* **2000**, *122*, 3797−3798.

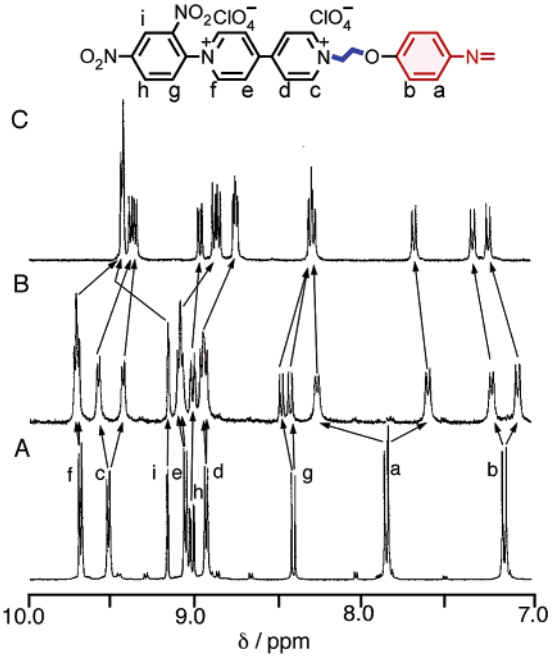

Figure 1. The ^{1}H NMR spectra of **1-ref** in DMSO-d_6 (A) at 30 °C and **1** in DMSO-d_6 (B) and D_2O (C) at 30 °C.

α-CyD moved from the azobenzene moiety to the methylene spacers in **2** (and **3**), a part of α-CyD may still interact with the azobenzene moiety, which hampers the photoisomerization due to steric hindrance. In contrast, the energy barrier is expected to be small in DMSO; thus, α-CyD allows moving from the azobenzene moiety to one propylene moiety as the secondary station beyond the viologen moiety. The observed behaviors indicate that **2** functions as a molecular shuttle driven by dual-stimuli, that is, light and solvent polarity. More details about the motion of α-CyD are described in Molecular Shuttling Driven by Light and Heating section.

The first-order rate constants (k_1) and thermodynamic parameters for the *cis*−*trans* thermal isomerization are expected to reflect the energy barrier arising from the rotaxane structure. The reaction of **1** and **1-ref** from the *cis*-form to the *trans*-form in the dark was examined. The k_1 values and activation parameters are summarized in Table 2. The influence of the rotaxane structure on the dark reaction can be estimated by comparing the activation parameters of **1** to those of **1-ref**. As can be seen in Table 2, the $\Delta S^{\ddagger}$ values of **1-ref** in water and DMSO are more negative by 11.7 and 24.8 J mol^{-1}·K^{-1} than those of **1**, respectively. In addition, the $\Delta S^{\ddagger}$ values of **1-ref** in water and DMSO are different, while those of **1** are almost the same. Solvation is known to affect the $\Delta S^{\ddagger}$ values.[43,44] The obtained results indicate that the transition state of the azobenzene moiety in **1-ref** is more solvated than that in **1**, for which solvation is hindered due to the existence of α-CyD. Despite the large difference in the $\Delta S^{\ddagger}$ values of **1** and **1-ref** in DMSO, their rate constants are almost the same. This is due to the compensation relation between $\Delta S^{\ddagger}$ and $\Delta H^{\ddagger}$.[43,44] In contrast, the rate constant of **1** in water is about 7-fold faster than that of **1-ref**. Moreover, the $\Delta H^{\ddagger}$ values are almost the same, and the $\Delta S^{\ddagger}$ terms are not compensated by the $\Delta H^{\ddagger}$ terms. It is known that *cis*-azobenzene is strongly stabilized in water by solvation.[45] Therefore, the compound **1-ref** in water is stabilized by the solvation, which reflects the rate constant,[46] whereas **1** prefers the *trans*-form since the *trans*-form is stabilized via the formation of the inclusion complex between α-CyD and the *trans*-form, which leads to the acceleration of the rate constant.

Molecular Shuttling Driven by Light and Heating. The shuttling processes of α-CyDs driven by light irradiation on **1** in water and **2** in DMSO were estimated using circular dichroism (CD) spectroscopy. The measurement conditions are almost the same as those stated in the section of Photoisomerization and Thermal Isomerization. The measurement temperature of the CD spectra of **1** was fixed at 5 °C, where the thermal isomerization during the measurement is negligible. As we previously described,[36] the CD spectra of an aqueous solution of **1** before photoirradiation show positive and negative induced CD (ICD) bands (see Figure 2B), which are assigned to the $\pi-\pi^*$ and n$-\pi^*$ transitions for *trans*-**1** at 360 and 430 nm, respectively. It is theoretically and experimentally known that the band for the ICD of the long axis polarized transitions of arene guests parallel to the axis of the CyD cavity is positive.[47,48] After irradiation with UV light (360 nm), the positive ICD band at 360 nm decreases together with the increase in the positive ICD band at 312 nm and the negative ICD band at 430 nm, which are assignable to the $\pi-\pi^*$ and n$-\pi^*$ transitions for *cis*-**1**, respectively. The induced CD bands (λ_{max} = 360 and 435 nm) of compound **7**, the thread compound of **1**, in the presence of α-CyD disappeared by the photoisomerization of the azobenzene moiety from the *trans*- to *cis*-forms (see Supporting Information, Figure S3). On the basis of the data described above, it is suggested that, for **1**, α-CyD exists close to the azobenzene unit when **1** is in the *cis*-form. Upon irradiation with visible light (430 nm), the spectrum of *cis*-**1** reverted to that of the *trans*-**1** with isosbestic points at 269 and 330 nm. The photoisomerization of the rotaxane **2** occurred in DMSO, but not in water as described in the section of Photoisomerization and Thermal Isomerization. Figure 2F shows the CD spectra of a DMSO solution of **2**. Before photoirradiation, a positive ICD peak, which is assignable to the $\pi-\pi^*$ transition for the *trans*-**2** at 330 nm was observed, while no n$-\pi^*$ transition band was seen. In contrast, the ICD bands assigned to the $\pi-\pi^*$ and n$-\pi^*$ transitions were observed in the CD spectra for the aqueous solutions of **1** (as described above) and **2** (Figure 2D). The presence of the n$-\pi^*$ transition band would be due to the difference in the positioning of α-CyD on the azobenzene unit. In water, α-CyD in *trans*-**1** is believed to remain only on the azo group due to the strong hydrophobic interaction, which induces the ICD band for the n$-\pi^*$ transition. On the other hand, in DMSO, the location of α-CyD in *trans*-**2** is expected to shift slightly from the azo group to the methylene moiety probably due to the formation of hydrogen bonding[10] as described in the section of Formation of Rotaxane Structure. This shift resulted in no ICD band of the n$-\pi^*$ transition. After irradiation with UV light (350 nm) on a DMSO solution of **2**, the positive ICD band at 330 nm decreased without the

(43) Shinkai, S.; Kusano, Y.; Shigematsu, K.; Manabe, O. *Chem. Lett.* **1980**, 1303−1306.
(44) Shinkai, S.; Nakaji, T.; Nishida, Y.; Ogawa, T.; Manabe, O. *J. Am. Chem. Soc.* **1980**, *102*, 5860−5865.
(45) Halpern, J.; Brady, G. W.; Winkler, C. A. *Can. J. Res.* **1950**, *28B*, 140−155.
(46) Sanchez, A. M.; de Rossi, R. H. *J. Org. Chem.* **1996**, *61*, 3446−3451.
(47) Shimizu, H.; Kaito, A.; Hatano, M. *Bull. Chem. Soc. Jpn.* **1979**, *52*, 2678−2684.
(48) Ueno, A.; Fukushima, M.; Osa, T. *J. Chem. Soc., Perkin Trans. 2* **1990**, 1067−1072.

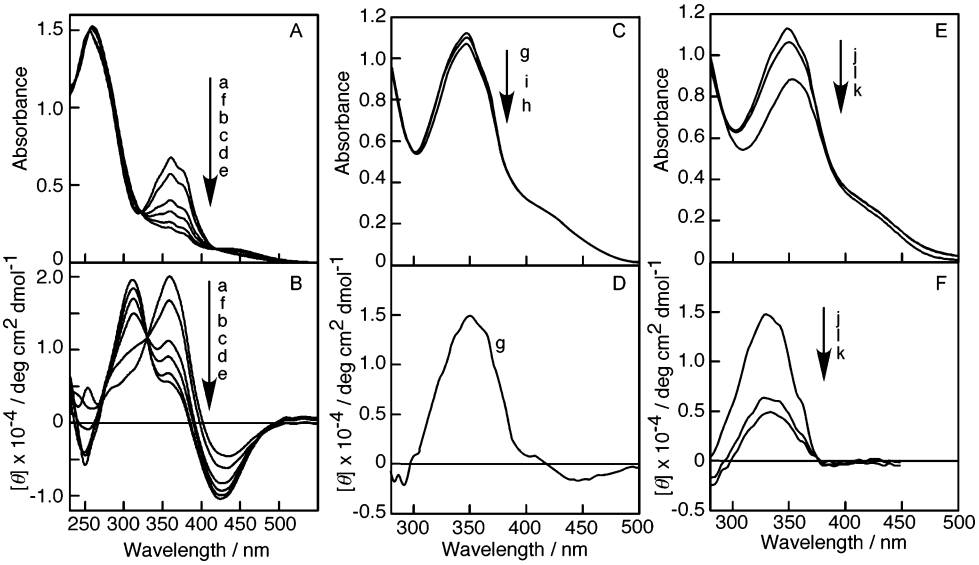

Figure 2. The UV−visible (A) and CD (B) spectra of **1** in water at 5 °C and the UV−visible (C and E) and CD (D and F) spectra of **2** in water (C and D) and in DMSO (E and F) at 20 °C. [**1**] = [**2**] = 2.0×10^{-4} mol dm^{-3}. The irradiation times of UV light (350 nm) are 0 (a, g, j), 2.0 (b), 4.0 (c), 8.0 (d), 13 (e), and 20 min (h, k). The spectra f, i, and l were obtained by visible light irradiation (420 nm) for 14 min (f) and 20 min (i, l) after the measurement of e, h and k, respectively.

Table 1. The Photoisomerization Ratios[a] of the Rotaxanes at Specified Temperatures

	Rotaxane **1**[b]		Rotaxane **2**[b]		Rotaxane **3**[b]	
temperature (°C)	H_2O	DMSO	H_2O	DMSO	H_2O	DMSO
5	67%	*c*		*c*		*c*
20	74%	17%	<2%	25%		
30	62%	68%			∼0	∼0

[a] Photoisomerization ratios for the generation of the *cis*-forms of the rotaxanes were calculated from the decrease in the absorbance at 350 nm, where the absorbance of the *cis*-form is negligible. [b] [**1**] = [**2**] = [**3**] = 2.0×10^{-5} mol dm^{-3}. [c] The temperature is below the melting point of DMSO (18.5 °C).

Table 2. The First-Order Rate Constants (k_1) and Activation Parameters for the Isomerization from *cis*- to *trans*-Forms in **1** and **1-ref** in the Dark[a]

	Rotaxane **1**		**1-ref**	
	H_2O	DMSO	H_2O	DMSO
k_1 ($\times 10^4$) (s^{-1})[b]	2.9	0.91	0.43	1.1
$\Delta G^{\ddagger}_{303}$ (kJ mol^{-1})[b]	94.8	97.7	99.6	97.1
$\Delta H^{\ddagger}$ (kJ mol^{-1})	84.2	87.7	85.5	79.6
$\Delta S^{\ddagger}$ (kJ mol^{-1}·K^{-1})	−34.8	−33.1	−46.5	−57.9

[a] [**1**] = [**1-ref**] = 2.0×10^{-5} mol dm^{-3}. [b] Data at 303 K.

appearance of a new band near 420 nm (Figure 2F), suggesting the moving of α-CyD from the azobenzene moiety to the secondary station far from the azobenzene in *cis*-**2**. With visible light (430 nm) irradiation, the UV−visible spectrum of *cis*-**2** reverts to that of *trans*-**2**; however, the CD band near 350 nm recovered only 15% of the pristine CD band of *trans*-**2**. This means that α-CyD still locates at the secondary station even after the visible light irradiation. The obtained results reveal that (i) the shuttling of α-CyD in **1** is driven by light, and (ii) the shuttling of **2** can be controlled by two parameters, that is, light and solvent polarity.

Dynamic NMR spectroscopy[49] was carried out to examine the movement of α-CyD by heating **1** in water and **2** in DMSO.

(49) Sandstöm, J. *Dynamic NMR Spectroscopy*; Academic Press: London, 1982; pp 79−84.

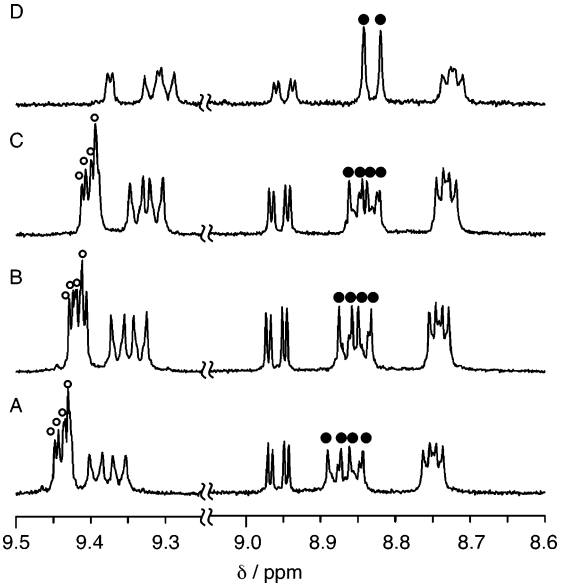

Figure 3. The ^{1}H NMR spectra of a D_2O solution of **1** at 5 (A), 30 (B), 55 (C), and 80 °C (D).

Figure 3 shows the data in the range of 5−80 °C for an aqueous solution of **1**. Accompanying the temperature increase from 5 to 55 °C, the signals of the viologen units shifted slightly due to the enhancement of the molecular motion of the viologen moieties, in which the chemical shifts for the protons of the azobenzene moiety were almost constant, indicating that α-CyD remains on the azobenzene unit in the temperature range of 5−80 °C. At 80 °C, the signals (denoted by the open circle in Figure 3) of the viologens at 9.45 ppm disappeared, and the two paired doublet signals (denoted by the closed circle in Figure 3) became two paired singlet signals. This suggests that a D−H exchange reaction took place at the protons (proton f in Figure 1) on the viologen moieties in **1**. To confirm the possibility of D−H exchange, we prepared bis(2,4-dinitrophenyl)bipyridinium dichloride as the model compound of **1**. The ^{1}H NMR spectrum of this compound after heating in D_2O at 80 °C for 1 h showed

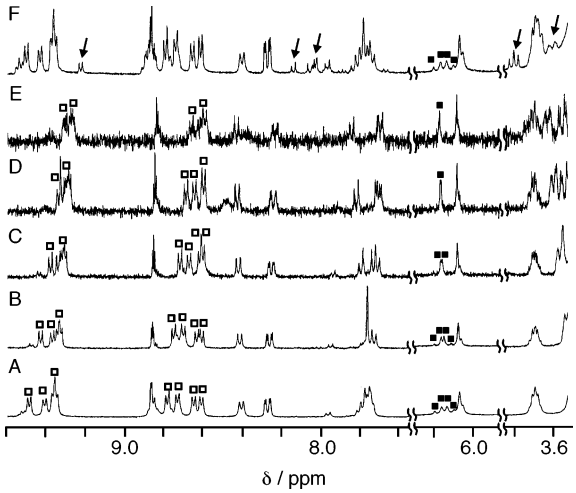

Figure 4. The ^{1}H NMR spectra of a DMSO-d_6 solution of **2** at 30 (A), 60 (B) 90 (C), 120 (D), and 150 °C (E), and then, at 30 °C (F) after the measurement of E.

that the peak intensities of a doublet signal assignable to the four protons next to the nitrogen on the bipyridinium moiety and the paired doublet signal decreased and a new singlet signal appeared at 8.98 ppm. The molecular weights of bis(2,4-dinitrophenyl)bipyridinium dichloride before and after the heating obtained by FAB-MS measurements was 490.2 and 493.2, respectively, suggesting that the D−H exchange of three protons in the four protons next to the nitrogen on the bipyridinium moiety occurred. The acidity enhancement of the protons by the introduction of 2,4-dinitrophenyl groups might cause the D−H exchange.

In contrast, a coalescence of the split signals in the spectra was observed for a DMSO solution of **2** at the temperature range of 90−150 °C (Figure 4). We considered that the coalescence comes from shuttling of α-CyD along the long axis of **2**. However, we have to be careful for the decomposition of the compound at such high temperatures, so we have conducted a HPLC (Hitachi, L-7100) experiment to detect α-CyD that should be released by the decomposition of compound **2**. The column used was Cosmosil Sugar-D (Nakarai Tesque Inc.), and the eluent was acetonitrile/water (65/35, v/v). It was found that only a trace amount of α-CyD was detected for a DMSO-d_6 solution of **2** after heating to 150 °C. Therefore, we can conclude that the decomposition of **2** is negligible in our experimental condition. At 90 °C, the double-doublet signal (denoted by a closed square) at 6.15 ppm that is assignable to the methylene becomes a singlet signal. This means that the geminal protons of the one methylene are equivalent on the NMR time scale. At 150 °C, the eight doublet signals of the viologen moieties then changed to four broad signals. This means that the protons of the two viologen moieties exist in a similar environment. These coalescences are derived from the shuttling of α-CyD within the azobenzene moiety for the first step and then between the azobenzene moiety and the propylene moieties. When the temperature cycled back to 30 °C after heating to 150 °C, new signals with low intensities appeared in the spectra (denoted by the arrows in Figure 4). For example, the signals at 3.6 and 3.8 ppm in Figure 4F could be assignable to protons on the propylene moiety. The appearance of new signals derived from the movement of α-CyD from the azobenzene moiety to the propylene moieties is also evident. The activation free energy ($\Delta G^{\ddagger}$) and the rate constant at the coalescence temperature (k_c) were determined in order to investigate the movement of α-CyD in **2**. The rate constant of a site-exchange process at T_c is determined by the chemical shift between the target signals ($\Delta\upsilon$), which is used for the calculation of $\Delta G^{\ddagger}$ based on the Eyring equation.[49] From the double-doublet at 6.15 ppm for the one methylene, $\Delta\upsilon$ and J_{AB} are 25.2 and 13.7 Hz, respectively. The values k_c and $\Delta G^{\ddagger}$ at T_c (90 °C) for the first step were calculated to be 94 s^{-1} and 80 kJ mol^{-1}, respectively, and k_c at 30 °C extrapolated from the Eyring equation with the $\Delta G^{\ddagger}$ was estimated to be 0.53 s^{-1}. The slow rate constant at 30 °C for the first step would be due to the hydrogen bonding[10] between the hydroxy groups of α-CyD and the protons of the methylene spacer next to the pyridinium moiety (see Formation of Rotaxane Structure section). From the signals between 8.6 and 8.8 ppm for the one viologen, where $\Delta\upsilon$ is 51 Hz, the k_c and $\Delta G^{\ddagger}$ at 150 °C for the second step were calculated to be 111 s^{-1} and 88 kJ mol^{-1}, respectively. The value k_c at 30 °C was estimated to be 0.08 min^{-1}. Harada and co-workers reported the shuttling behavior of the rotaxane containing α-CyD as a ring and dodecamethylene units linked with viologens as a thread in DMSO.[18] They determined k_c at T_c (130 °C) and $\Delta G^{\ddagger}$ for slipping of the α-CyD on the viologen unit to be 80 s^{-1} and 85 kJ mol^{-1}, respectively, and k_c at 30 °C was estimated to be 0.9 min^{-1}. The rate constant for the slipping of α-CyD on the viologen unit in **2** is 10 times lower than that of Harada's rotaxane. The difference in the slipping behavior between **2** and Harada's rotaxane would be due to the difference in the their chemical structures; that is, Harada's rotaxane has a linear structure, and **2** is bent at the methylene spacers. The steric factor is expected to play an important role in the slipping of α-CyD through the viologen moieties.

The CD spectra for the DMSO solution of **2** after heating to the specified temperatures provided further evidence for the movement of α-CyD in **2** (see Supporting Information, Figure S4). Although the intensity of the ICD band of **2** was not much different than heating to 100 °C, by further heating to 140 °C, the CD intensity drastically decreased. This suggests that α-CyD slips through the viologen units to the propylene moieties.

To obtain further evidence that α-CyDs stay at their secondary stations in *cis*-**1** and **2** after heating to 120 °C, we employed NOE differential spectroscopy. As we described elsewhere,[36] after UV light irradiation, the NOE differential spectrum for an aqueous solution of **1**, in which the peak for the protons of the ethylene spacer as a secondary station at 5.30 ppm is perturbed, shows a negative NOE peak[50] at 3.65 ppm that is assignable to the H-3 and/or H-5 protons of α-CyD, which are directed toward the inside of the cavity (Figure 5A). This is evidence showing that, after UV light irradiation, α-CyD exists at the ethylene spacer moiety in **1**. A DMSO solution of **2** at room temperature after heating to 120 °C also gives a negative NOE peak at 3.37 ppm that is assignable to the H-3 and/or H-5 protons of α-CyD, when the peak for the protons of the middle methylene in the propylene spacer as the secondary station at 2.38 ppm was perturbed (Figure 5B). Furthermore, the ^{1}H NMR spectrum of a DMSO solution of **2** at 30 °C after UV light irradiation shows a new signal at 3.78 ppm that is assignable to the methylene next to NH in the propylene units. The appearance of new

(50) Abraham, R. J.; Fisher, J.; Loftus, P. *Introduction of NMR Spectroscopy*; John Wiley & Sons: New York, 1988.

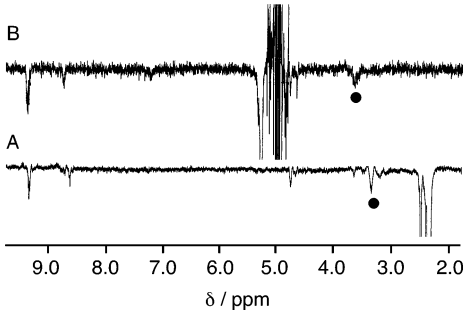

Figure 5. The NOE differential spectra for (A) a D_2O solution of **1** at 5 °C after UV light irradiation and (B) for a DMSO-d_6 solution of **2** at 30 °C after heating to 120 °C. The signal of the methylene spacer at 5.38 ppm for **1** and the signal of the middle methylene in the propylene spacer at 2.38 ppm for **2** were perturbed.

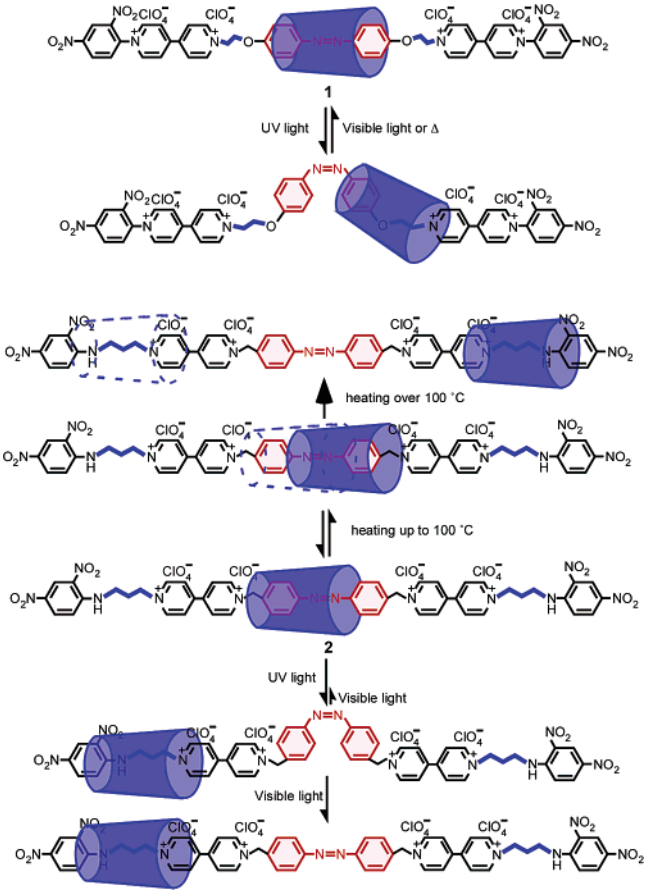

Figure 6. Schematic drawing for the shuttling processes of **1** and **2**.

signals was also observed in the NMR spectra at 30 °C after heating to 120 °C (Figure 4F). This result suggests that α-CyD exists at the propylene spacer moiety in *cis*-**2** and **2** after heating to 120 °C.

Figure 6 is a schematic drawing for the shuttling processes of **1** and **2**. In rotaxane **1**, α-CyD reversibly moves between the azobenzene moiety and the ethylene spacer moiety by the alternating photoirradiation of UV and visible light or temperature (from *cis*-**1** to *trans*-**1**). In rotaxane **2**, α-CyD moves within the azobenzene moiety at the temperatures below 100 °C and moves though the axis of the rotaxane at temperatures above 100 °C. By UV light irradiation, the α-CyD in **2** also moves from the azobenzene moiety to the propylene spacer moiety. However, the shuttling process by the alternating photoirradiation of UV light and visible light is irreversible.

Conclusions

We have described the design, synthesis, and the molecular shuttling behavior of rotaxanes **1**−**3**, which consist of α-CyD as a ring, azobenzene as a photoactive moiety and a primary station, viologen as a hydrophilic group and an energy barrier for the slipping of α-CyD, and 2,4-dinitrobenzene as a stopper. The ^{1}H NMR and CD spectral measurements clarified that **1**−**3** form rotaxane structures, in which the α-CyD stays on the azo group in **1**−**3** in water, and on one methylene moiety in **2** (and **3**) in DMSO. The UV−visible spectral measurements have revealed that **1** shows a reversible isomerization between the *trans*- and *cis*-forms of the azobenzene moiety in both water and DMSO by alternating irradiation of the UV and visible lights, whereas the photoisomerization of **2** occurs in DMSO, but not in water. For **3**, the photoisomerization occurs neither in water nor in DMSO. The influence of the rotaxane structure on the first rate constants and thermodynamic parameters for the *cis*−*trans* thermal isomerization of **1** is greater in water than in DMSO since the presence of α-CyD hampers the solvation by water. The CD and NOE differential spectral measurements for the photochemically driven molecular shuttling processes of **1** in water and **2** in DMSO demonstrated that α-CyD in **1** moves reversibly from the azobenzene moiety to the ethylene moieties via the alternating photoirradiation of the UV and visible lights. The reversible movement of α-CyD in **2** from/to the azobenzene moiety to/form the propylene spacers also occurs. The dynamic NMR, NOE differential, and CD spectroscopies clearly indicated that α-CyD in **2** in DMSO shuttles (i) within the azobenzene moiety at temperatures below 100 °C, and (ii) between the azobenzene moiety and the propylene moieties at temperatures above 100 °C. The rates of both shuttling processes are slow possibly due to the formation of some hydrogen bonding[10] between the hydroxy groups of α-CyD and the protons on the methylene next to the viologen moieties and the bending structure of **2**. We reached the conclusion that the molecular shuttling processes for **1** and **2** are driven by three different modes, that is, by light for **1** and heating and solvent polarity for **2**.

The stimuli used are orthodox; however, they provide a powerful technique for controlling and monitoring the molecular shuttling processes. The present study would afford the opportunity to design and develop nanoscale switching devices based on multi-mode-driven molecular shuttles.

Experimental Section

General Methods. 4,4′-Bipyridyl, 2,4-dinitrofluorobenzene, 1,2-dibromoethane, *p*-hydroxyacetanilide, and 3-bromopropylamine hydrobromide were purchased from Tokyo Kasei, Inc. α-Cyclodextrin was purchased from Wako Pure Chemical Inc. These reagents were used as received. Solvents were purchased from Kishida Chemical Co., LTD, unless indicated otherwise. Dimethylformamide was dried over CaH_2 and distilled prior to use, and other solvents for the synthesis were distilled prior to use. Dimethyl sulfoxide used in the measurements was of spectral grade. Water was purified through an Ultrapure water system, Milli-Q Plus (Millipore Co.). Its resistivity was over 18 MΩ cm. Deuterated solvents were purchased from Merck LTD and Euriso-Top SA. All other chemicals used were of reagent grade. 4,4′-Bis(2-chloromethyl)azobenzene was synthesized according to the literature.[40]

^{1}H and NOE differential NMR spectra were recorded on a JEOL JNM-GX400 NMR in the presence of internal standards (TMS or DSS). The UV−visible and circular dichroism (CD) spectral measurements were carried out on a Hitachi U-3000 spectrophotometer and a JASCO J-720 spectropolarimeter, respectively. Temperatures were maintained to be constant within ±0.1 °C (Neslab Instruments, Inc., Circulator RTE−100). Photoirradiation for *trans*−*cis* photoisomerization of the rotaxanes and the corresponding reference compounds was performed on a spectrofluorometer (JASCO FP-770, light source: 150 W xenon lamp). The slit width used in the experiment was 20 nm. The sample concentration for the UV−visible spectral and circular dichroism (CD) spectral measurements was 2.0×10^{-5} mol dm^{-3}. FAB-MS and TOF-MS spectral measurements were conducted on a JEOL JMS-700N and an Applied Biosystems Voyager-DE Pro, respectively.

Photoisomerization ratios for the generation of *cis*-forms of the rotaxanes were calculated from the decrease in the absorbance at around 350 nm, where the absorbance of the *cis*-form is negligible. The reactions reached the photostationary states within 15 min. The rate constants of the regeneration of the *trans*-forms from the *cis*-form in the dark were determined by monitoring the increase in the absorption band of the *trans*-form at around 350 nm. The OD plotted against reaction time satisfied the first-order equation with $r > 0.999$. $\Delta H^{\ddagger}$ and $\Delta S^{\ddagger}$ were determined from linear plots of $\Delta G^{\ddagger}$ against T, where $\Delta G^{\ddagger}$ at the given temperatures was calculated with Eyring equation

$$k_1 = \kappa \frac{k_B T}{h} \exp\left(\frac{-\Delta G^{\ddagger}}{RT}\right)$$

where k_1, k_B, and h are the first-order rate, and Bolzmann and Planck constants, respectively.

On dynamic NMR study,[49] rate constants (k_c) at T_c and for the first step (an AB system) and the second step are written by the approximate equations

$$k_c = \pi[0.5\{(\Delta\nu)^2 + 6J_{AB}{}^2\}]^{1/2}$$

and

$$k_c = \frac{\pi}{\sqrt{2}}\Delta\nu^2$$

respectively, where $\Delta\nu$ and J_{AB} are the difference in the chemical shift between the target split signals and coupling constant, respectively.

Eyring equation was used to calculate $\Delta G^{\ddagger}$ at the coalescence temperature and to extrapolate values of k at 30 °C. $\Delta G^{\ddagger}$ was obtained at 10% error range since many approximations are involved in this semiquantitative treatment.

4-(2-Bromoethoxy)acetanilide (4). A mixture of *p*-hydroxyacetanilide (2.0 g, 13.3 mmol), 1,2-dibromoethane (25 g, 133 mmol), and tetrabutylammonium perchlorate (0.09 g, 0.26 mmol) in a saturated aqueous solution of sodium carbonate (12 mL) was vigorously stirred at 80 °C for 28 h. After evaporation of excess amount of 1,2-dibromoethane and water, the residue was extracted with chloroform (50 mL) and an insoluble solid (1,2-bis(4-acetamidophenoxy)ethane) was filtered off. The extract was washed twice with a saturated aqueous solution of sodium carbonate (50 mL), dried over anhydrous $MgSO_4$, filtered, and then evaporated to dryness. The resulting solid was recrystallized twice from ethanol/water to give **4** as a white solid (1.4 g, 40%). Mp 127 °C. Found: C, 46.84; H, 4.70; N, 5.58%. Calcd for $C_{10}H_{12}BrNO_2$: C, 46.53; H, 4.69; N, 5.43%. ^{1}H NMR (300 MHz, CD_3-OD, TMS): δ 7.43 (d, 2H, ArH), 6.88 (d, 2H, ArH), 4.27 (t, 2H, ethylene), 3.66 (t, 2H, ethylene), 2.09 (s, 3H, CH_3) ppm. IR (KBr) 1658 ($\nu_{C=O}$) cm^{-1}.

4-(2-Bromoethoxy)-4′-hydroxyazobenzene (5). A solution of **4** (2.5 g, 9.7 mmol) in ethanol containing 20−30 wt % of HBr was refluxed for 24 h. After evaporation of the solvent, the resulting light-brown solid was used for next reaction without further purification.

To a suspension of the brown solid in 1 M HCl aqueous solution (126 mL) was added dropwise a solution of $NaNO_2$ (0.75 g, 10.9 mmol) in water (5 mL) at 0 °C to result in a transparent solution in a few minutes. Excess amount of $NaNO_2$ was quenched with sulfamic acid by monitoring the iodostarch reaction. After the separation of a small amount of insoluble parts by filtration, the mother liquid was added dropwise to a solution of phenol (1.25 g, 13.4 mmol) and Na_2CO_3 (2.5 g, 23.6 mmol) in water (25 mL) at 0 °C. The solution immediately became an ocherous suspension. After stirring for 1 h, the suspension was adjusted to pH 4 with glacial acetic acid. The ocherous solid was filtered off, washed with a large amount of water, and then recrystallized twice from hexane then acetone to obtain **5** as a ocherous solid (2.8 g, 90%). Mp 147 °C. MS (EI) *m*/*z* 321 [M$^+$]. ^{1}H NMR (300 MHz, $CDCl_3$, TMS): δ 7.85 (m, 4H, ArH), 7.02 (d, 2H, ArH), 6.94 (d, 2H, ArH), 5.34 (s, 1H, OH), 4.36 (t, 2H, ethylene), 3.67 (t, 2H, ethylene) ppm. IR (KBr) 3409 (ν_{OH}), 1594 ($\nu_{N=N}$) cm^{-1}.

4,4′-Bis(2-bromoethoxy)azobenzene (6). To a suspension of **5** (2.5 g, 7.8 mmol), 1,2-dibromoethane (15.6 g, 81.2 mmol), and tetrabutylammonium perchlorate (0.07 g, 0.2 mmol) was added dropwise a saturated Na_2CO_3 (10 mL) aqueous solution at 80 °C. After stirring for 32 h at 80 °C, 1,2-dibromoethane was removed under reduced pressure, and then the residue was extracted twice with chloroform (each 20 mL portion). The chloroform solutions were combined, washed with water, dried over anhydrous $MgSO_4$, filtered, and then evaporated to dryness. The crude solid was recrystallized twice from chloroform/ethanol (1/2 v/v) to obtain **6** as a yellow solid (1.7 g, 50%). Mp 156 °C. Found: C, 45.18; H, 3.73; N, 6.53%. Calcd for $C_{16}H_{16}Br_2N_2O_2$: C, 44.86; H, 3.77; N, 6.54%. ^{1}H NMR (300 MHz, $CDCl_3$, TMS): δ 7.86 (d, 4H, ArH), 7.03 (d, 4H, ArH), 4.37 (t, 4H, ethylene), 3.68 (t, 4H, ethylene) ppm. IR (KBr) 1594 ($\nu_{N=N}$) cm^{-1}.

4,4′-Bis(4-(4′-pyridyl)pyridinium-2-ethoxy)azobenzene dibromide (7). A solution of **6** (0.2 g, 0.47 mmol) and 4,4′-bipyridyl (0.4 g, 2.2 mmol) in dry DMF (3 mL) was stirred for 24 h at 75 °C. A precipitate generated was filtered off and washed with DMF and diethyl ether to obtain **7** as a yellow solid (0.2 g, 57%). Mp 262 °C. Found: C, 57.95; H, 4.43; N, 10.82%. Calcd for $C_{36}H_{32}Br_2N_6O_2$+0.5H_2O: C, 57.69; H, 4.44; N, 11.21%. ^{1}H NMR (300 MHz, DMSO-d_6, TMS): δ 9.32 (d, 4H, PyH), 8.87 (d, 4H, PyH), 8.70 (d, 4H, PyH), 8.06 (d, 4H, PyH), 7.84 (d, 4H, ArH), 7.14 (d, 4H, ArH), 5.14 (t, 4H, ethylene), 4.67 (t, 4H, ethylene) ppm. IR (KBr) 1600 ($\nu_{N=N}$) cm^{-1}.

4,4′-Bis(4-(4′-(2,4-dinitrophenyl)pyridinium)pyridinium-2-ethoxy)-azobenzene tetraperchlorate (1-ref). A solution of **7** (1.0 g, 1.3 mmol), 2,4-dinitrofluorobenzene (2.4 g, 13.0 mmol), and tetrabutylammonium perchlorate (0.01 g) in water (60 mL) was stirred for 24 h at 25 °C. The aqueous reaction mixture was washed twice with chloroform and added sodium perchlorate (5.0 g) to precipitate **1-ref** as a yellow solid (0.8 g, 48%). Mp 229 °C. Found: C, 43.79; H, 2.94; N, 10.40%. Calcd for $C_{48}H_{38}Cl_4N_{10}O_{26}$: C, 43.90; H, 2.92; N, 10.67%. TOF-MS (α-CHCA) *m*/*z* 1313.62 [(M + H)$^+$]. ^{1}H NMR (300 MHz, DMSO-d_6, TMS): δ 9.70 (d, 4H, PyH), 9.53 (d, 4H, PyH), 9.18 (d, 2H, ArH), 9.07 (d, 4H, PyH), 9.03 (dd, 2H, ArH), 8.95 (d, 4H, PyH), 8.42 (d, 2H, ArH), 7.86 (d, 4H, ArH), 7.16 (d, 4H, ArH), 5.23 (t, 4H, ethylene), 4.73 (t, 4H, ethylene) ppm. IR (KBr) 1600 ($\nu_{N=N}$), 1550, 1340 (ν_{NO2}) cm^{-1}.

Rotaxane 1. A solution of **7** (1.0 g, 1.3 mmol), 2,4-dinitrofluorobenzene (2.4 g, 13.0 mmol), and α-cyclodextrin (6.3 g, 6.5 mmol) in water (60 mL) was stirred for 24 h at 25 °C. The aqueous reaction mixture was washed twice with chloroform, added ammonium hexafluorophosphate (5.0 g), and then evaporated. Acetonitrile was added to the residue to remove an excess amount of the cyclodextrin. Tetraethylammonium chloride (5.0 g) was added to the resulting acetonitrile solution to produce a precipitate. After filtration, the solid product was resolubilized in water and reprecipitated by sodium perchlorate (5.0 g) to obtain **1** as a yellow solid (0.9 g, 30%). Mp 195 °C. Found: C, 43.57; H, 4.69; N, 6.11%. Calcd for $C_{84}H_{95}Cl_4N_{10}O_{56}$: C, 43.51; H, 4.30; N, 6.04%. TOF-MS (α-CHCA) *m*/*z* 1885.69 [(M − 4ClO_4)$^+$].

^{1}H NMR (300 MHz, D_2O, TMS): δ 9.43 (m, 6H, PyH, ArH), 9.35 (d, 2H, PyH), 9.32 (d, 2H, PyH), 8.95 (dd, 2H, ArH), 8.87 (d, 2H, PyH), 8.83 (d, 2H, PyH), 8.75 (d, 2H, PyH), 8.73 (d, 2H, PyH), 8.29 (d, 2H, ArH), 8.27 (d, 2H, azoArH), 7.68 (d, 2H, azoArH), 7.32 (d, 2H, azoArH), 7.21 (d, 2H, azoArH), 5.27 (m, 4H, ethylene), 4.96 (d, 6H, CyD), 4.85 (t, 2H, ethylene), 4.78 (t, 4H, ethylene), 3.8−3.5 (m, 36H, CyD) ppm. IR (KBr) 3400 (ν_{OH}), 1600 ($\nu_{N=N}$), 1550, 1340 (ν_{NO2}) cm^{-1}.

4-(4′-Pyridyl)-3-aminopropylpyridinium bromide hydrobromide (8). A solution of 4,4′-bipyridyl (7.13 g, 46 mmol) and 3-bromopropylamine hydrobromide (1.0 g, 4.6 mmol) in acetonitrile (100 mL) was refluxed for 1.5 h. After cooling, a precipitate generated was filtered and recrystallized from ethanol to give **8** as a white solid (1.0 g, 58%). Mp 223 °C. Found: C, 38.73; H, 4.88; N, 10.06%. Calcd for $C_{13}H_{17}N_3Br_2+1.6H_2O$: C, 38.66; H, 5.04 N, 10.40%. ^{1}H NMR (300 MHz, methanol-d_4, TMS): δ 9.22 (dd, 2H, PyH), 8.85 (dd, 2H, PyH), 8.58 (dd, 2H, PyH), 8.03 (dd, 2H, PyH), 4.84 (t, 2H, CCH_2Py), 3.15 (m, 2H, NCH_2), 2.45 (m, 2H, $CH_2CH_2CH_2$) ppm. IR (KBr) 3442 (ν_{NH}) cm^{-1}.

4,4′-Bis(4-(4′-(3-aminopropyl)pyridinium)pyridiniummethyl)-azobenzene dibromide(dichloride) bis(hydrobromide) (9). A solution of **8** (0.16 g, 2.4 mmol) and 4,4′-bis(chloromethyl)azobenzene (0.1 g, 0.36 mmol) in dry DMSO (5 mL) was stirred at 70 °C for 3.5 h. A precipitate generated was filtered and then washed with a large amount of DMSO and small amount of acetone to give **9** as a yellow solid (0.16 g, 86%). Found: C, 43.10; H, 4.65; N, 9.98%. Calcd for $C_{40}H_{46}N_8Cl_2Br_4+4.5H_2O$: C, 43.33; H, 4.98; N, 10.11%. ^{1}H NMR (300 MHz, D_2O, TMS): δ 9.29 (d, 4H, PyH), 9.23 (d, 4H, PyH), 8.69 (d, 8H, PyH), 8.08 (d, 4H, azoArH), 7.80 (d, 4H, azoArH), 4.95 (t, 4H, CCH_2-Py), 3.28 (t, 4H, NCH_2), 2.58 (m, 4H, $CH_2CH_2CH_2$) ppm. IR (KBr) 3430 (ν_{NH}) cm^{-1}.

4,4′-Bis(4-(4′-(3-(2,4-dinitrophenylamino)propyl)pyridinium)-pyridiniummethyl)azobenzene tetraperchlorate (2-ref). A solution of **9** (0.3 g, 0.3 mmol) and 2,4-dinitrofluorobenzene (1.5 g, 8.2 mmol) in dry DMF (40 mL) was stirred at 50 °C for 2 h. The solvent was evaporated, and then the crude product was washed with a large amount of chloroform and then methanol to produce **2-ref** as an orange solid (0.12 g, 30%). Mp 200 °C (dec). Found: C, 43.38; H, 3.63; N, 11.48%. Calcd for $C_{52}H_{48}Cl_4N_{12}O_{24}+3.6H_2O$: C, 43.62; H, 3.86; N, 11.74%. TOF-MS (α-CHCA) m/z 968.67 [(M − 4ClO$_4$)$^+$]. ^{1}H NMR (400 MHz, DMSO-d_6, TMS): δ 9.54 (d, 4H, PyH), 9.36 (d, 4H, PyH), 8.85 (s, 2H, ArH), 8.78 (d, 4H, PyH), 8.73 (d, 4H, PyH), 8.27 (d, 2H, ArH), 7.96 (d, 4H, azoArH), 7.82 (d, 4H, azoArH), 7.27 (d, 2H, ArH), 6.06 (s, 4H, methylene), 4.77 (t, 4H, CCH_2Py), 3.67 (t, 4H, NCH_2), 2.37 (m, 4H, $CH_2CH_2CH_2$) ppm. IR (KBr) 1610 ($\nu_{N=N}$), 1522, 1338 (ν_{NO2}) cm^{-1}.

Rotaxane 2. A mixture of α-cyclodextrin (2.0 g, 2.1 mmol) and **9** (0.25 g, 0.24 mmol) in water (40 mL) was stirred at room temperature for 10 min, followed by the addition of 2,4-dinitrofluorobenzene (0.9 g, 4.9 mmol) and then 0.1 M NaOH aqueous solution to adjust to pH 9−10. After stirring at 40 °C for 184 h, the reaction mixture was washed with 10 mL portions of chloroform four times to extract an excess amount of 2,4-dinitrofluorobenzene. Sodium perchlorate (4.0 g, 33 mmol) was added to the aqueous layer, and then the resulting gummy crude product was washed with a large amount of water then methanol to obtain rotaxane **2** as an orange solid (62 mg, 68%). Mp 200 °C (dec). Found: C, 43.57; H, 4.74; N, 7.42%. Calcd for $C_{88}H_{108}Cl_4N_{12}O_{54}+3.5H_2O$: C, 43.99; H, 4.82; N, 6.99%. TOF-MS (α-CHCA) m/z 1940.64 [(M − 4ClO$_4$)$^+$]. ^{1}H NMR (400 MHz, DMSO-d_6, TMS): δ 9.49 (d, 2H, PyH), 9.41 (d, 2H, PyH), 9.36 (m, 4H, PyH), 8.87 (s, 2H, ArH), 8.86 (m, 2H, NH), 8.80 (d, 2H, PyH), 8.74 (d, 2H, PyH), 8.66 (d, 2H, PyH), 8.61 (d, 2H, PyH), 8.41 (d, 2H, azoArH), 8.38 (dd, 2H, ArH), 7.78 (m, 6H, azoArH), 7.77 (d, 2H, ArH), 6.15 (m, 2H, methylene), 6.08 (s, 2H, methylene), 5.32 (d, 6H, CyDOH), 5.19 (s, 6H, CyDOH), 4.77 (t, 4H, CCH_2Py), 4.68 (d, 6H, CyDC1H), 4.27 (t, 6H, CyDOH), 3.67 (t, 4H, NCH_2), 3.46 (m, 12H, CyDC6H), 3.4−3.1 (m, 24H, CyDCH), 2.37 (m, 4H, $CH_2CH_2CH_2$) ppm. IR (KBr) 1610 ($\nu_{N=N}$), 1523, 1334 (ν_{NO2}) cm^{-1}.

4,4′-Bis(4-(4′-pyridyl)pyridiniummethyl)azobenzene dichloride (10). A solution of 4,4′-bis(chloromethyl)azobenzene (0.5 g, 1.8 mmol) and 4,4′-bipyridyl (1.29 g, 8.3 mmol) in dry DMF (30 mL) was stirred for 12 h at 85 °C. A precipitate generated was filtered off and washed with DMF and diethyl ether to obtain **10** as an orange solid (0.2 g, 57%). Mp 262 °C. Found: C, 63.81; H, 5.03; N, 13.13%. Calcd for $C_{34}H_{28}N_6Cl_2+2.5H_2O$: C, 64.14; H, 5.22; N, 13.20%. ^{1}H NMR (300 MHz, DMSO-d_6, TMS): δ 9.44 (dd, 4H, PyH) 8.88 (dd, 4H, PyH), 8.70 (dd, 4H, PyH), 8.04 (dd, 4H, PyH), 7.95 (dd, 4H, ArH), 7.84 (dd, 4H, ArH), 6.04 (s, 4H, methylene) ppm. IR (KBr) 1600 ($\nu_{N=N}$) cm^{-1}.

4,4′-Bis(4-(4′-(2,4-dinitrophenyl)pyridinium)pyridiniummethyl)-azobenzene tetraperchlorate (3-ref). A solution of **10** (0.3 g, 0.5 mmol) and 2,4-dinitrofluorobenzene (2.2 g, 12.0 mmol) in water (30 mL) was stirred for 44 h at 40 °C. The reaction mixture was washed twice with chloroform and then was added sodium perchlorate (2.0 g) to precipitate **3-ref** as an orange solid (0.45 g, 71%). Mp 170 °C (dec). Found: C, 43.02; H, 3.07; N, 10.79%. Calcd for $C_{46}H_{34}Cl_4N_{10}O_{24}+1.8H_2O$: C, 42.99; H, 2.95; N, 10.99%. TOF-MS (α-CHCA) m/z 854.75 [(M − 4ClO$_4$)$^+$]. ^{1}H NMR (400 MHz, DMSO-d_6, TMS): δ 9.69 (d, 4H, PyH), 9.60 (d, 4H, PyH), 9.18 (s, 2H, ArH), 9.04 (d, 4H, PyH), 9.03 (dd, 2H, ArH), 8.93 (d, 4H, PyH), 8.42 (d, 2H, ArH), 7.94 (d, 4H, azoArH), 7.80 (d, 4H, azoArH), 6.08 (s, 4H, methylene) ppm. IR (KBr) 1600 ($\nu_{N=N}$), 1550, 1340 (ν_{NO2}) cm^{-1}.

Rotaxane 3. A solution of **9** (0.75 g, 1.3 mmol), 2,4-dinitrofluorobenzene (2.4 g, 13.0 mmol), and α-cyclodextrin (6.3 g, 6.5 mmol) in water (50 mL) was stirred for 39 h at 25 °C. The reaction mixture was washed with chloroform three times. After the addition of ammonium hexafluorophosphate (5.0 g), the solvent was evaporated. Acetonitrile was added to the residue to remove an excess amount of the cyclodextrin. Tetraethylammonium chloride (4.0 g) was added to the acetonitrile solution to produce a precipitate, which was collected and dissolved in water, and then tetraethylammonium chloride was added to give a precipitate, which was collected and washed with methanol to give pure **3** as an orange solid (0.1 g, 4%). Mp 200 °C (dec). Found: C, 42.36; H, 4.39; N, 6.01%. Calcd for $C_{82}H_{94}Cl_4N_{10}O_{54}+5.0H_2O$: C, 42.53; H, 4.53; N, 6.05%. TOF-MS (α-CHCA) m/z 1826.50 [(M − 4ClO$_4$)$^+$]. ^{1}H NMR (300 MHz, D_2O, TMS): δ 9.33−9.12 (m, 6H, PyH), 9.20 (d, 2H, PyH), 8.84 (dd, 1H, ArH), 8.83 (dd, 1H, ArH), 8.75−8.70 (m, 4H, PyH), 8.65 (d, 2H, PyH), 8.63 (d, 2H, PyH), 8.37 (d, 2H, azoArH), 8.18 (d, 1H, ArH), 8.16 (d, 1H, ArH), 7.84 (d, 2H, azoArH), 7.80 (d, 2H, azoArH), 7.71 (d, 2H, azoArH), 6.10 (s, 2H, methylene), 6.02 (s, 2H, methylene), 4.86 (s, 6H, CyD), 3.63−3.36 (m, 36H, CyD) ppm. IR (KBr) 3400 (ν_{OH}), 1600 ($\nu_{N=N}$), 1535, 1335 (ν_{NO2}) cm^{-1}.

Acknowledgment. We thank Dr. M. Kimura and Dr. T. Fukuda of Nagasaki University for the helpful discussions on the dynamic NMR spectroscopy. This work was supported by Grants-in-Aid from the Ministry of Education, Science, Sports, and Culture, Japan.

Supporting Information Available: The ^{1}H NMR, UV−vis and CD spectra of **3**, CD spectra of **7** and **2**, and complete ref 12. This material is available free of charge via the Internet at http://pubs.acs.org.

JA053690L